Self-Assembled Polystyrene-*block*-poly(ethylene oxide) Micelle Morphologies in Solution

Prachur Bhargava,[†] Joseph X. Zheng,[†] Pei Li,[‡] Roderic P. Quirk,[†] Frank W. Harris,[†] and Stephen Z. D. Cheng*,[†]

The Maurice Morton Institute and Department of Polymer Science, The University of Akron, Akron, Ohio 44325-3909, and Department of Applied Biology and Chemical Technology, The Hong Kong Polytechnic University, Hung Hom, Kowloon, Hong Kong, P.R. China

Received March 25, 2006; Revised Manuscript Received May 6, 2006

ABSTRACT: We have investigated the self-assembly behavior of an amphiphilic diblock copolymer, polystyrene-*block*-poly(ethylene oxide) (PS-*b*-PEO), in *N*,*N*-dimethylformamide (DMF)/water and DMF/acetonitrile. In both cases water and acetonitrile are selective solvents for the PEO block. The degrees of polymerization of the PS and PEO blocks were 962 and 227 (PS_{962}-*b*-PEO_{227}), respectively. Micelle morphologies of the block copolymer in both systems could be controlled by varying copolymer and selective solvent concentrations. With increasing the water concentration in the DMF/water or the acetonitrile concentration in the DMF/acetonitrile system, the micelle morphology observed in transmission electron microscopy changed from spheres to wormlike cylinders and then to vesicles. The morphological diagrams were constructed from the study of the micelle morphology changes in different copolymer concentrations and the critical micellization concentrations for both systems at different copolymer concentrations as determined by static light scattering experiments. In between the concentration regions of two neighboring pure micelle morphologies, mixed morphologies such as spheres with short cylinders or wormlike cylinders with vesicles could be found. Although the trend in morphological changes was identical in these two systems, there were remarkable differences in the morphological diagrams of PS_{962}-*b*-PEO_{227} with respect to the percentage of selective solvent added. This is due to the large difference between the polymer-selective solvent interaction parameters. On the basis of the observations of morphological reversibility and annealing experiments, these two morphological diagrams were proven to be in thermodynamic equilibrium. The driving force for these morphological changes was understood to approach micelle free energy minimization. Approximate micelle free energy calculations confirmed that the free energy decreases as the morphology changes from spheres to wormlike cylinders and then to vesicles with an increase in the selective solvent concentrations. Possible change mechanisms are also discussed.

Introduction

Amphiphilic block copolymers can self-assemble to form micelles in aqueous media or when mixed with organic solvents.[1−8] Micelles of block copolymers, which have a long corona and small core, are termed as "starlike", while the ones with a large core and short corona are termed as "crew cut".[9] A plethora of morphologies have been recently reported, pioneered by Eisenberg and other research groups, some of which are analogous to those formed by small molecule amphiphiles, such as surfactants.[10−16] Symmetric micelles, in which the core- and corona-forming blocks are similar in size, can also form multiple micelle morphologies.[16] These self-assembled colloidal systems are important due to their specific applications,[17] such as in colloidal drug delivery,[18,19] as emulsifying agents, and in separation systems.[17]

Parameters to control the morphology and size of the self-assembled micelles can be divided into two categories: molecular and solution parameters. First, the molecular parameters include the chemical nature of repeating units of the blocks, the size of each block, the overall molecular weight, and the architecture. It has been shown in the past decade that these parameters are key tuning the micelle morphologies.[13,14] The second category, which has been investigated only recently, includes the type of solvents and solvent quality, the solvent/nonsolvent ratio, the copolymer concentration, the pH value, additives such as salts, ions, and homopolymer, and the temperature.[20,21] The micelle morphology is also sometimes tuned by introducing specific interactions like hydrogen bonding or excess chirality in the monomer units.[22]

The micelle morphologies, which have been obtained by varying one or more of the above parameters, include but are not limited to spheres, cylinders, wormlike, helical,[22] bilayers, vesicles, and others.[23] The formation of different morphologies is explained by considering the micelle free energy, which consists of three components:[24] the free energy of the core, which relates to the stretching of the core-forming block; the free energy of the interface, which relates to the surface tension between the core-forming block and the solvent; and the free energy of the corona, to which the electrostatic and steric interactions of the corona-forming blocks contribute.

The preparation methods for these micelle morphologies have a variety of routes depending on individual systems. Starlike micelles can usually be prepared by direct dissolution of a block copolymer in a selective solvent for one of the blocks. In this way, the polymer−solvent interaction parameter, χ_{P-S}, does not vary. Another method involves heating of a selective solvent to dissolve both hydrophilic and hydrophobic blocks and then cooling the system to form micelles. For crew-cut micelle formation in diblock copolymers, when the block forming the core is glassy at the preparation temperature, direct dissolution cannot be used. The copolymer has to be first dissolved in a common solvent. One example is polystyrene-*block*-poly(acrylic

[†] The University of Akron.
[‡] The Hong Kong Polytechnic University.
* To whom correspondence should be addressed. E-mail: scheng@uakron.edu.

10.1021/ma060677s CCC: $33.50
Published on Web 06/15/2006

acid) (PS_{310}-*b*-PAA_{52}) dissolved in dioxane. Then, a selective solvent, water, is added slowly to induce micellization.[20] A systematic study of the micelle morphology changes of this copolymer with increasing water concentration in a dioxane/water mixture has also been carried out.[25] The χ_{P-S} in this method changes continuously as the selective solvent is added. Micelle morphologies in other systems have also been reported using this method.[11,21,23]

We are interested in micellization of polystyrene-*block*-poly(ethylene oxide) (PS-*b*-PEO) diblock copolymers. This was first investigated almost four decades ago in a selective solvent for the PS block.[26] In 1982, spherical micelles in water, which is a selective solvent for the PEO block, were studied via static light scattering experiments.[27] Recently, the micellization of PS-*b*-PEO in the presence of various additives was also reported.[28,29] Eisenberg and co-workers obtained multiple micelle morphologies of PS-*b*-PEO by either adding millimolar amounts of salts or acid[12] or by varying the molecular weight of the PEO block.[30] In both cases, the block copolymers were sufficiently crew cut. In most cases, different mixed micelle morphologies were observed. A pure single morphology was rarely found. Using a similar method, complex bilayer aggregates including tubules, which were dependent on the relative block length, polymer concentration, and annealing time, were also seen.[31,32] More recently, by changing the common solvent they observed a "vesicle with hollow rods", which was identified to be a trapped intermediate morphology.[33,34] The effect of polymer architecture and common solvent on micelle morphologies of PEO-*b*-PS-*b*-PEO triblock copolymers was also reported.[35]

The purpose of our research is to investigate the effect of copolymer concentration and the solvent quality on crew-cut micelle morphologies and their changes in PS_{962}-*b*-PEO_{227}, which has, so far, not been carried out systematically. We have used the approach of dissolving the copolymer in *N*,*N*-dimethylformamide (DMF) and then adding water or acetonitrile, which are selective solvents for the PEO block. Therefore, two solvent systems (DMF/water and DMF/acetonitrile) for this diblock copolymer have been investigated. The micelle morphologies are directly visualized under transmission electron microscopy (TEM). The critical micellization concentrations have been determined by light scattering experiments.

Experimental Section

Sample Synthesis and Preparations The diblock copolymer PS_{962}-*b*-PEO_{227} was synthesized using living anionic polymerization based on a standard route which is published elsewhere.[36] In brief, the PS precursor was characterized by size exclusion chromatography (SEC) using polystyrene standards and had a number-average molecular weight of 100K g/mol (the degree of polymerization of ~962) and a polydispersity of 1.03. The number-average molecular weight of PEO blocks was determined by proton nuclear magnetic resonance to be 10K g/mol (the degree of polymerization of ~227). A polydispersity of 1.04 in the overall copolymer was determined by SEC using the universal calibration. The volume fraction of PS blocks (f_V^{PS}) was 0.914. The PS_{962}-*b*-PEO_{227} was first dissolved in anhydrous DMF by stirring at room temperature for a few days to obtain stock solutions of different copolymer concentrations (0.1−8 wt %), and they were then sealed with Teflon tape and stored at room temperature. Anhydrous DMF was filtered through a filter of 0.02 μm pore size before making the stock solutions.

The method for preparing solutions was similar in both systems. The difference was only in how fast the selective solvent was added and how long the samples were equilibrated. In the DMF/water system, each ~10 mL of stock solution was taken in a vial, and deionized water was added dropwise to reach a predetermined DMF/water ratio. The contents of the vial were stirred continuously to allow rapid mixing of DMF and water. Each drop added was ~0.1 wt % water of the total solution weight, and at least a 30 min gap was kept between adding consecutive drops. After the predetermined DMF/water ratio was reached, solutions were sealed and left to equilibrate for a period of time between 6 and 8 h and up to several days with mild stirring. This process was repeated to obtain micellar solutions with different DMF and water ratios. After equilibrating the solutions, they were left standing without stirring for at least 30 min before taking the samples for micelle morphological observations. In the DMF/acetonitrile system, ~1 wt % acetonitrile of the total solution weight was added every 10 min. The samples were then sealed and equilibrated at least overnight before preparing the samples for morphological observations.

Equipments and Experiments. Micelle morphological observations were performed on a TEM (Philips TECNAI) with an accelerating voltage of 120 kV. To observe micelle morphologies under TEM yet retain the original morphological sizes and geometries as in the solution, a small amount of solution was "quenched" in excess water (≥100 times) to quickly vitrify the PS blocks into its glassy state, and then a drop from the quenched solution was placed on a carbon-coated grid. After a few minutes, the excess solution was blotted away with filter paper. The grids were dried at room temperature and atmospheric pressure for several hours before examination in the TEM. Since the PS blocks were in their glassy state, the "quenched" morphologies were kept in TEM.[20] Alternatively, the quenched samples were also placed in dialysis tubes and dialyzed against distilled water for 4 days to remove DMF. Distilled water was changed twice a day. The dialyzed aqueous solutions were then used to prepare the sample for TEM observations. Using both methods to prepare the samples, identical results were obtained.

To determine the critical micellization concentration (cmc), static light scattering experiments were conducted using a Brookhaven Instrument coupled with a BI-200SM goniometer, BI-9000AT correlator, and an EMI-9863 photomultiplier tube for photon counting. A Meller Griot 35 mW He−Ne laser was used as light source (632.8 nm). A cylindrical glass scattering cell with a diameter of 12 mm was placed at the center of a thermostated bath (±0.01 °C) with decahydronaphthalene used for refractive index matching. The measurements were carried out at 90° scattering angle at 25 °C. The glass scattering cells were extensively cleaned by ultrasonication in THF and ethanol to eliminate any dust and impurity. The stock solutions were filtered into the scattering cells through filters of 0.45 μm pore size. Water or acetonitrile was added dropwise through filters of 0.02 μm pore size.

Results and Discussion

Morphological Diagrams. Figure 1 shows a set of TEM images of the micelle morphologies for 0.1 wt % initial PS_{962}-*b*-PEO_{227} concentration in the DMF/water system. At a low water concentration of 2.75 wt %, the micelles are spherical (Figure 1a). They change to mixed spheres and short cylinders (the length <400 nm) at a water concentration of 3.14 wt % (Figure 1b). At a water concentration of 3.54 wt % as shown in Figure 1c, the mixed spheres and cylinders can still be observed. However, the length of the cylindrical micelles becomes increasingly long (several micrometers) with a decreased population of spheres. Sometimes, the pearl necklace morphology is also observed to coexist. At a water concentration of 4.17 wt %, a morphological change occurs to form exclusively long wormlike micelles (Figure 1d). On further increasing the water concentration to 4.24 wt %, mixed wormlike micelles and vesicles appear (Figure 1e). Finally, the morphology changes to exclusively vesicles at a water concentration of 4.52 wt % (Figure 1f). If water is added further, the morphology does not change and we observed vesicles even when water is added up

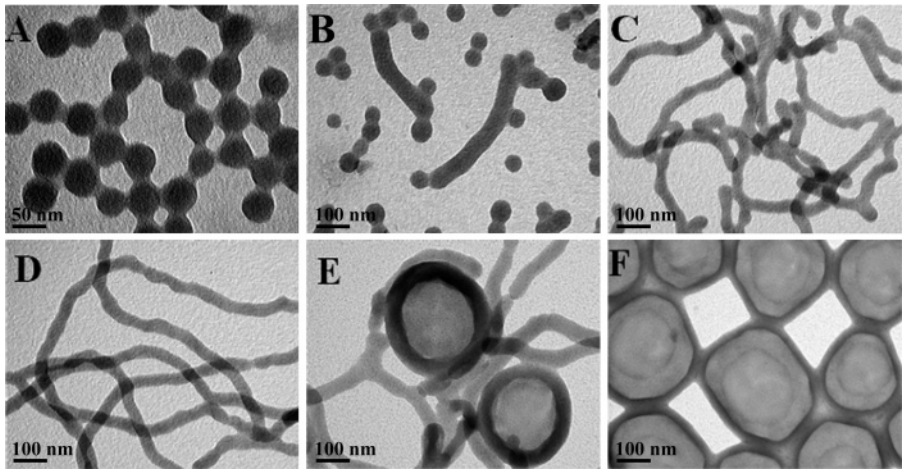

Figure 1. Morphological transitions with adding water in the DMF/water system for initial copolymer concentration of 0.1 wt %: (a) a pure sphere morphology at 2.75 wt % water; (b) a mixed spheres and rods at 3.14 wt % water; (c) a mixed spheres and long rods at 3.54 wt % water; (d) a pure wormlike morphology at 4.17 wt % water; (e) a mixed wormlike and vesicles at 4.24 wt % water; and (f) a pure vesicle morphology at 4.52 wt % water.

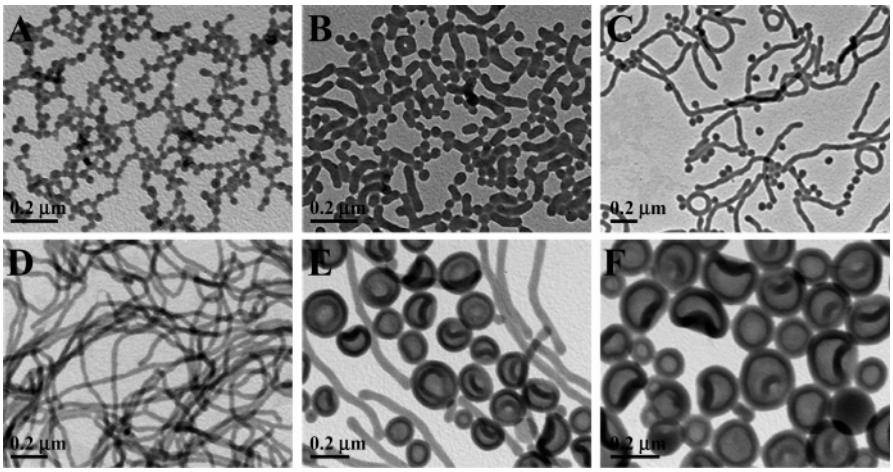

Figure 2. Morphological transitions with adding acetonitrile in the DMF/acetonitrile system for initial copolymer concentration of 0.5 wt %: (a) a pure sphere morphology at 8 wt % acetonitrile; (b) a mixed spheres and rods at 16 wt % acetonitrile; (c) a mixed spheres and long rods at 30 wt % acetonitrile; (d) a pure wormlike morphology at 37 wt % acetonitrile; (e) a mixed wormlike and vesicles at 45 wt % acetonitrile; and (f) a pure vesicle morphology at 70 wt % acetonitrile.

to 50 wt %. We believe that polystyrene blocks are frozen at much lower water contents (~10 wt %) due to its hydrophobic nature, and thus the morphology does not change further. From TEM observations, the distribution of wall thickness of the vesicles seems to become narrow at higher water contents; therefore, by varying the water concentration in a region between 2.75 and 4.52 wt %, the micelle morphologies of PS_{962}-*b*-PEO_{227} undergo controlled changes which are very sensitive to the small increment in water concentration.

In the system of PS_{962}-*b*-PEO_{227} in DMF/acetonitrile for an initial copolymer concentration of 0.5 wt %, Figure 2 shows a set of TEM images of the micelle morphologies. The PS_{962}-*b*-PEO_{227} block copolymer first forms spheres at a low acetonitrile concentration of 8 wt % (Figure 2a). The micelle morphology changes to mixed spheres and cylinders in the acetonitrile concentrations between 16 and 30 wt % (Figure 2b,c), to wormlike cylinders at 37 wt % (Figure 2d), then to mixed cylinders and vesicles at 45 wt % (Figure 2e), and finally to vesicles at 70 wt % (Figure 2f). Therefore, the micelle morphology changes take place in a much broader region of the acetonitrile concentration between 8 and 70 wt %. On adding acetonitrile further, the morphology does not change and remains as vesicles. At these higher acetonitrile contents (>70 wt %), we expect the mobility of PS blocks would be severely restricted, as acetonitrile is bad solvent for PS, and thus, the morphology may not change.

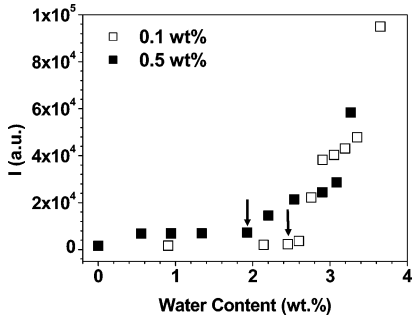

Figure 3. Static light scattering measurements with adding water in the DMF/water system. The arrows point out the cmc at different initial copolymer concentrations.

To construct micelle morphological diagrams of these two systems, we need systematic investigations of these changes with respect to different initial copolymer and selective solvent concentrations. Light scattering experiments were utilized to determine the cmc for the diagrams. In the system of PS_{962}-*b*-PEO_{227} in DMF/water, Figure 3 shows that the cmc for 0.1 wt % initial copolymer concentration is at 2.5 wt % of water, and for 0.5 wt % initial copolymer concentration, the cmc is at 1.9

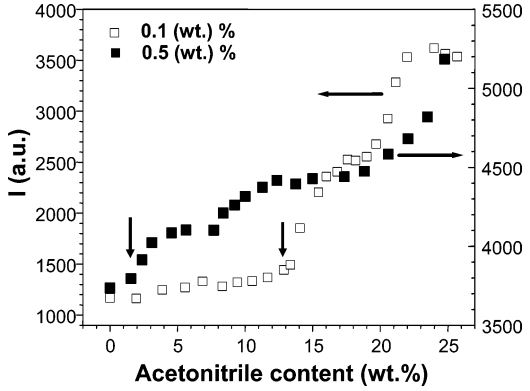

Figure 4. Static light scattering measurements with adding acetonitrile in the DMF/acetonitrile system. The arrows point out the cmc at different initial copolymer concentrations.

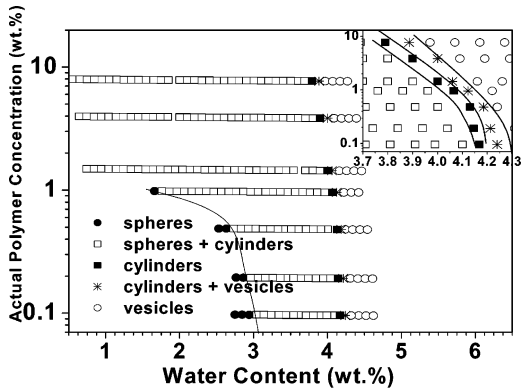

Figure 5. Morphological change diagram for PS_{962}-*b*-PEO_{227} in the DMF/water system.

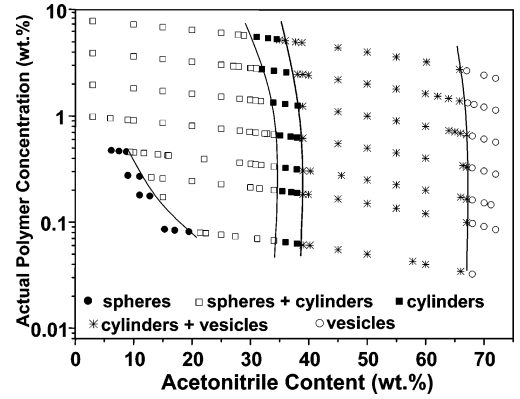

Figure 6. Morphological change diagram for PS_{962}-*b*-PEO_{227} in the DMF/acetonitrile system.

wt % of water (the arrows in Figure 3). On the other hand, in the system of PS_{962}-*b*-PEO_{227} in DMF/acetonitrile, the light scattering experiments in Figure 4 show that for 0.1 wt % initial copolymer concentration the cmc is at 13 wt % of acetonitrile, and for 0.5 wt % initial copolymer concentration, the cmc is at 2 wt % of acetonitrile (the arrows in Figure 4). On adding acetonitrile further to this solution, we observe that the scattered intensity shows further jumps at certain acetonitrile concentrations. The position of these jumps closely coincides with the acetonitrile concentrations where we observe morphological changes in TEM. Thus, these jumps in the scattered intensity could be related to the morphological changes.

Figures 5 and 6 show two morphological diagrams for the DMF/water and DMF/acetonitrile systems, respectively, in a region of initial PS_{962}-*b*-PEO_{227} concentrations from 0.1 to 8 wt %. In this study, TEM is the primary technique utilized to construct these diagrams. The morphological boundaries in these two figures are drawn using lines between the data points of different micelle morphologies. In the case of the DMF/water system, the successive points are taken with small increments of the water concentration, since the morphology is very sensitive to the amount of water added into this system. For the DMF/acetonitrile system, the increment of successive data points is relatively large in terms of the acetonitrile concentration. Smaller increments are used only near the morphological change regions in order to obtain more accurate observations for determining the morphological boundaries.

Note that in the DMF/water system the selective solvent concentration changes within several percentages to induce the micelle morphological changes from spheres to wormlike cylinders and then to vesicles, while in the DMF/acetonitrile system, the selective solvent changes within several ten percentages to complete the micelle morphological changes. Yet both systems possess the identical pathway of morphological changes with increasing the selective solvent concentrations (Figures 5 and 6). The morphological changes in both systems also shift to lower selective solvent concentrations as the initial PS_{962}-*b*-PEO_{227} concentration increases.

The question is, what is the reason for this vast difference in selective solvent concentrations between these two systems where the morphological changes occur? As the selective solvent is added, the solvent becomes progressively poorer for the micelle core formed by the PS blocks. Quantitatively, the poorness of the selective solvent with respect to the PS block is determined by the PS−solvent interaction parameter, if we neglect the entropic contribution. These parameters can be estimated using the van Laar−Hildebrand equation of[37]

$$\chi_{P-S} = [V_S/(RT)](\delta_P - \delta_S)^2 \quad (1)$$

where V_S is the molar volume of the solvent and δ_P and δ_S are solubility parameters of the polymer and selective solvent, respectively. Since the solubility parameter of PS is 9.04 $(cal/cm^3)^{0.5}$, while that of water is 23.4 $(cal/cm^3)^{0.5}$ and acetonitrile is 11.9 $(cal/cm^3)^{0.5}$,[37] the χ_{P-S} values for both systems can be calculated as $\chi_{PS-water} = 6.27$ and $\chi_{PS-acetonitrile} = 0.73$. The $\chi_{PS-water}$ value is close to 9 times higher than the $\chi_{PS-acetonitrile}$ value, indicating that water is a much poorer solvent for PS as compared to acetonitrile. Adding a small amount of water can result in a substantial increase in the interfacial free energy to initiate the micellization. This is equivalent to adding a large amount of acetonitrile. The increase in the interfacial free energy leads to an increase in the micelle size and thus an increase of the stretching of the PS blocks in the core. This ultimately gives rise to the morphological changes. The breadths of morphological changes and the regions of stabilized morphologies can thus be tuned by choosing appropriate selective solvents.

An attempt was made to make a reduced plot for both morphological diagrams without success. The reason may be due to the solvent interaction difference between DMF/water and DMF/acetonitrile which has not been taken into consideration.

Thermodynamic and Kinetic Aspects of the Morphological Changes. The criteria for achieving stable morphologies are that the obtained morphologies must be stable over a long period of time, and the morphological changes due to varying the selective solvent concentration must be reversible.[25] The question is whether the morphological changes in Figures 5 and 6 are the thermodynamic phase diagrams. In other words, does the rate of adding selective solvent affect the morphological changes? It is known that the evolution toward equilibrium

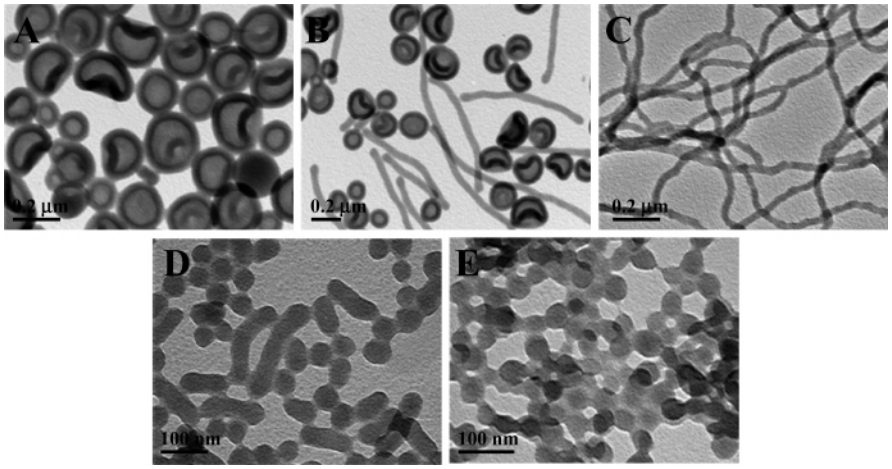

Figure 7. Reversible morphological changes by adding DMF into the DMF/acetonitrile system with 0.6 wt % initial copolymer concentration and 68 wt % acetonitrile: (a) the original micelle morphology is pure vesicle; (b) mixed wormlike and vesicles at 50 wt % of acetonitrile; (c) a pure wormlike morphology at 37 wt % acetonitrile; (d) mixed spheres and rods at 25 wt % acetonitrile; and (e) a pure sphere morphology at 7 wt % acetonitrile.

micelle morphologies depends on mobility of the core-forming blocks, which are associated with the solubility of the amphiphilic diblock copolymer in the solvent.[38] In general, our experience is that the rate of adding selective solvents must be slow enough and the amount of selective solvent added each time must be small enough in order to obtain the stable micelle morphologies.

The micelle morphologies observed in Figures 5 and 6 are stable over months as long as the systems are kept closed. To further prove that the micelle morphologies obtained are truly in thermodynamic equilibrium, we designed two sets of experiments. First, we chose to add DMF into a DMF/acetonitrile system with an initial PS_{962}-*b*-PEO_{227} concentration of 0.6 wt % and an acetonitrile concentration of 68 wt %. Figure 7 shows a set of TEM images of the micelle morphological changes after slowly adding different amounts of DMF. Figure 7a is the initial vesicle morphology of the system. Adding DMF to this system leads to the formation of mixed wormlike cylinders and vesicles at 50 wt % acetonitrile (Figure 7b), wormlike cylinders at 37 wt % acetonitrile (Figure 7c), mixed spheres and cylinders at 25 wt % acetonitrile (Figure 7d), and spheres at 13 wt % acetonitrile (Figure 7e). In this experiment, the rate of adding DMF is critical. When the DMF concentration is initially low (the acetonitrile concentration is high), the mobility of PS block is severely restricted, and thus, DMF has to be added slowly (1 wt % increment of the total solution weight per 10 min). When the DMF concentration becomes gradually high, DMF can be added at a faster rate (1 wt % increment of the total solution weight per 1 min). Figure 7 thus reveals that the micelle morphological changes are reversible.

Second, we examine the thermodynamic stability of the morphologies by adding the selective solvent quickly to generate kinetically "quenched" morphologies. We then carried out "annealing" experiments to monitor whether these kinetically generated morphologies return to the thermodynamically stable morphology. We started with a system that had 1 wt % initial PS_{962}-*b*-PEO_{227} concentration in pure DMF; the selective solvent acetonitrile was added at a fast rate (1 wt % increment of the total solution weight per 1 min) to reach an acetonitrile concentration of 35 wt %. The "quenched" morphology formed is mixed spheres and cylinders as shown in Figure 8a. Note that, on the basis of Figure 6, this system should display a stable morphology of wormlike cylinders. The system was then annealed at room temperature for 1 month; the mixed morphology gradually changes to wormlike cylinders, as shown in Figure 8b. Therefore, the wormlike cylinders should be the thermodynamically stable morphology.

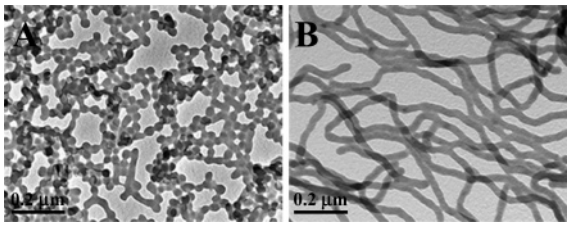

Figure 8. Morphologies formed by a fast rate of acetonitrile addition to a 1 wt % initial copolymer solution in DMF. Acetonitrile was added to 35 wt % (a) after 1 day and (b) after 1 month.

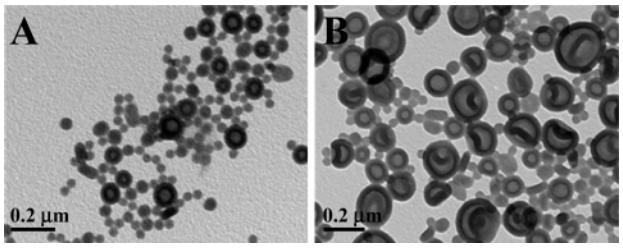

Figure 9. Morphologies formed by a fast rate of acetonitrile addition to a 2 wt % initial copolymer solution in DMF. Acetonitrile was added to 68 wt % (a) after 1 day and (b) after 2 months.

In another experiment for a system with 2 wt % of the initial PS_{962}-*b*-PEO_{227} concentration in pure DMF, the selective solvent of acetonitrile was added at a fast rate (1 wt % increment of the total solution weight per 1 min) to an acetonitrile concentration of 68 wt %. "Quenched" morphology of mixed spheres and vesicles is observed as shown in Figure 9a. Note that, on the basis of Figure 6, this system should display a morphology of pure vesicles. We annealed the system for 2 months at room temperature; the mixed morphologies can be observed to be in the process of returning to vesicles, as shown in Figure 9b. The annealing time of 2 months is apparently not long enough to completely reach the stable vesicles. We can thus conclude that although a fast rate of adding selective solvent may form kinetically "quenched" micelle morphologies (in most cases, they are mixed morphologies), the thermodynamically stable morphology can always be recovered as long as the PS blocks are not in their glassy state and the system is annealed for a sufficient time. The appropriate equilibrium time required to

Table 1. Micelle Size and Calculated Parameters for a 0.5 wt % Initial Copolymer Concentration at Three Selective Solvent Concentrations

	solvent concn (wt) %		diam or wall thickness (nm)		S_c (stretching)		s (area per chain, nm^2)		reduced tethering density	
morphology	water	AN[a]	water	AN[a]	water	AN[a]	water	AN[a]	water	AN[a]
spheres	2.63	7.5	48.5 ± 4.0	42.5 ± 2.9	1.14 ± 0.08	1.01 ± 0.06	19.8 ± 1.2	22.6 ± 1.2	3.4 ± 0.2	3.0 ± 0.2
cylinder	4.18	37.9	35.5 ± 2.2	38 ± 3.4	0.84 ± 0.04	0.9 ± 0.06	18.1 ± 1.1	16.9 ± 1.5	3.7 ± 0.2	4.1 ± 0.3
lamella	4.34	68.0	26.5 ± 3.3	34.6 ± 1.9	0.62 ± 0.06	0.81 ± 0.04	12.1 ± 0.8	9.3 ± 0.5	5.5 ± 0.6	7.2 ± 0.4

[a] AN stands for acetonitrile.

recover the thermodynamically stable morphologies is dependent on the chain dynamics, which is in turn dependent on the molecular weight of the chains and the solvent composition.[25] At high acetonitrile content the chain dynamics would be slow as compared to low acetonitrile content, as acetonitrile is a bad solvent for polystyrene, and the friction forces would also increase as the micelle core would be less swollen.[39] Thus, the annealing time required to recover the thermodynamically stable morphologies is dependent on the concentration of acetonitrile in our system.

Estimation of Micelle Free Energies. To further understand the reasons for the appearance of micelle morphological changes from spheres to wormlike cylinders, to vesicles in different selective solvent and initial PS_{962}-*b*-PEO_{227} concentrations, free energies in each of these micelle morphologies must be estimated. In these micelles, the PS blocks form the core and the PEO blocks form the corona.[40] We have utilized the size and geometry data which are obtained from the TEM images as the first approximation. (The precise calculation needs the size and geometry of micelles in solution.) The first parameter which needs to be calculated is the degree of stretching of PS blocks in the core (S_c) based on the equation[24]

$$S_c = R/R_0 \tag{2}$$

where R is the radius of the PS core in the spheres or in the wormlike cylinders. In the case of vesicles, R is half of the wall thickness. The quantity R_0 is the unperturbed end-to-end distance of a PS chain which can be calculated from the following equation[34]

$$R_0 = 0.067M^{0.5} \tag{3}$$

where M is the number-average molecular weight of the PS block. We approximate the observed micelle radius to be the radius of the PS cores, since in our case the PS block composition is much higher as compared to PEO composition (f_V^{PS} is 0.914). Furthermore, the PEO coronas are collapsed during the preparation of the samples for the TEM observations.

The second parameter is the interfacial area per chain (s). It can be calculated on the basis of the following equations[24]

$$s_{sphere} = 3V_S N_{PS}/(f R_{core}) \tag{4a}$$

$$s_{cylinder} = 2V_S N_{PS}/(f R_{core}) \tag{4b}$$

and

$$s_{lamella} = V_S N_{PS}/(f R_{lamella}) \tag{4c}$$

where f is the volume fraction of PS blocks in the core, V_S is the volume of PS monomer, and N_{PS} is the degree of polymerization of the PS block. Note that we use $R_{lamella}$ (half the wall thickness) to approximate the calculation in the case of vesicles. If we assume sufficiently dense PS blocks in the core, f approaches unity. The value of f would be closer to unity when the selective solvent concentrations are high as compared to when selective solvent concentrations are low. The observed dimensions and the calculated parameters based on eqs 1−4 for both DMF/water and DMF/acetonitrile systems for 0.5 wt % initial copolymer concentrations are listed in Table 1 at three representative selective solvent concentrations (where the pure micelle morphologies appear). As the morphology changes from spheres to wormlike cylinders, to vesicles, both the S_c and s values decrease.

Since the corona can be considered as tethered chains on a convex or quasi-planar substrate, the strength of corona repulsion can also be evaluated by the reduced tethering density, $\tilde{\sigma}$, which is defined as[41−43]

$$\tilde{\sigma} = \pi R_g^2/s \tag{5}$$

where s is the interfacial area per chain and R_g is the radius of gyration of the tethered PEO chains in the specific solution. The R_g value in this study is calculated using a scaling law reported in water at room temperature by Devanand and Selser.[44] This scaling law also predicted a correct R_g value of PEO for a particular molecular weight in DMF.[45] We thus used this scaling law to approximate the R_g values for PEO in good solvents. The $\tilde{\sigma}$ values listed in Table 1 increase from 3 to 7.2 as the morphology changes. This implies that the coronas in this study start approaching the boundary between the noninteraction and crossover regimes in spheres and pass the onset of the chain overcrowding to enter the crossover regime to generate some repulsion in vesicles. They are far away from the highly stretched brush regime.[41−43]

The total free energy of one chain in a micelle is

$$F = F_{core} + F_{interface} + F_{corona} \tag{6}$$

Let us consider each of these components individually. The term F_{core} is the elastic free energy of the core and can be estimated by the degree of stretching S_c in the core[46]

$$F_{core}/kT = k_j S_c^2 \tag{7a}$$

The coefficient k_j has been calculated for the case of dense cores: $k_{sphere} = 3\pi^2/80$, $k_{cylinder} = \pi^2/16$, and for the case of lamellae $k_{lamella} = \pi^2/8$.[47] As shown in Table 1, $S_c < 1$ in some cases. This may be due to two reasons. First, during the preparation of TEM samples using excess water the micelles could deswell and reduce the degree of stretching of the PS blocks and/or, second, there might be a possibility that the chains could actually be compressed, especially when the solvent quality becomes increasingly poor for the cores. In a recent study by SAXS and cryo-TEM for PS-*b*-PI block copolymer in solution, the value of S_c was found to be less than one in the case of vesicles.[48] Since eq 7a would predict a decrease in free energy even if the compression increases, we need to modify this equation so that it predicts an increase in the free energy when compression increases. If we define the degree of compression as $1/S_c$ and assume that the coefficient k_j is identical in compression as in stretching, we can modify eq 7a as

$$F_{core}/kT = k_j(1/S_c)^2 \quad (7b)$$

Therefore, eq 7a is applicable when the core is stretched, and eq 7b is applicable when core is compressed in our calculations.

The term $F_{interface}$ is related to the interfacial energy between the core (PS) blocks at the interface and the solvent. Therefore[46]

$$F_{interface} = \gamma s \quad (8a)$$

where s is the interfacial are per chain, which we have already determined, and γ is the surface tension, which is related to $\chi_{core-solvent}$ by the following expression[3,49,50]

$$\gamma = (kT/a^2)(\chi_{core-solvent}/6)^{0.5} \quad (8b)$$

where a is the PS monomer length. This expression originally derived for two homopolymers[49] has been regularly utilized in micellization theories.[3,50] The term $\chi_{core-solvent}$ for different solvent concentrations can be estimated using the solubility parameters[37] and respective volume fractions.

The term F_{corona} is based on the expression recently proposed by Zhulina et al. in their theory of diblock copolymer micelles.[46] When the corona is treated as chains tethered on a quasi-planar substrate, the upper-limit value of the F_{corona} values for these micelle morphologies can be provided, since all of these morphologies possess convex surface for the corona chains to be tethered onto, and thus, the chain stretching must be reduced in the real cases. This free energy expression is expressed by

$$F_{corona}/kT = \hat{C}_H \hat{C}_F N_{PEO}(sa^{-2})^{-1/2\nu} \quad (9a)$$

where N_{PEO} is the degree of polymerization of the PEO block, a is the PEO monomer length, and ν is the scaling exponent, which is equal to 3/5 for a good solvent. The $\hat{C}_H$ and $\hat{C}_F$ values are numerical prefactors, and in the case of a good solvent, they are

$$\hat{C}_H = C_H(l/a)^{1/3}\upsilon^{1/3} \quad (9b)$$

$$\hat{C}_F = C_F \quad (9c)$$

where C_H and C_F are model parameters which were calculated to be 0.68 and 1.38, respectively,[46] l is the Kuhn length, a is the PEO monomer length, and υ is the excluded volume parameter of PEO in the specific solvent. The values of l and a are 1.1 nm and 0.35 nm, respectively.[51,52] The excluded volume parameter υ is related to the second virial coefficient A_2[51]

$$\upsilon = 2A_2 M_0^2/(a^3 N_A) \quad (9d)$$

where M_0 is the molecular weight of the PEO monomer and N_A is Avogadro's number. The values of A_2 in the literature for our specific molecular weight and/or scaling laws have enabled us to determine the values of A_2 for PEO in DMF, in water, and in acetonitrile.[44,53−56] To calculate the values at different concentrations of the systems, we have further used the individual A_2 values and the volume fractions of the respective solvents. Using eqs 9a−9d, the free energy of the corona can therefore be calculated.

The calculated individual free energy components and the total free energy for a 0.5 wt % initial copolymer concentration at representative solvent concentrations (given in Table 1) are listed in Table 2. The total free energy decreases as the morphology changes from spheres to wormlike cylinders to vesicles. The F_{core}/kT increases from spheres to wormlike cylinders and then to vesicles as the chains are compressed. When $\chi_{core-solvent}$ increases, the $F_{interface}/kT$ decreases as the micelle size becomes increasingly large. The F_{corona}/kT increases as the reduced tethering density increases, leading to increased chain repulsions. However, both of the F_{core} and the F_{corona} values are much smaller compared to the $F_{interface}$, which is dominant.

In the above calculations, we have not considered the rim energy of the lamella as compared to closed vesicles. This rim energy is $E_{rim} = 2\pi R\gamma$, where R is the radius of the circular lamella and γ is the surface tension. For our system in the concentration region of forming vesicles, $\gamma \sim 2kT$ based on eq 8b; therefore, for a circular lamella with a radius of 200 nm, $E_{rim} \sim 800\pi kT$. This huge free energy increase can be avoided if the lamella closes to form vesicles. However, in bending the lamella to form a vesicle, a bending energy E_{bend} needs to be considered. In spherical vesicles the bending energy is independent of the size of the vesicle and is equal to $E_{bend} = 8\pi k_c$, where k_c is the bending modulus.[57,58] A typical value for block copolymer bilayers is $k_c \approx 40kT$ so that $E_{bend} \approx 320\pi kT$, a total energy required to bend a lamella to form a spherical vesicle. Quantitatively, for a circular lamella having a radius of 200 nm, the number of chains [the aggregation number (N_{agg})] can be calculated by[24]

$$N_{agg} = f\pi R^2 t/N_{PS}V_{PS} \quad (10)$$

where R is the radius of the lamella (200 nm), t is the wall thickness (~30 nm in our vesicles),V_{PS} is the volume of the PS repeating unit, and N_{PS} is the degree of polymerization of the PS block. If we assume a sufficiently dense PS core and f is close to unity, the N_{agg} is calculated to be 23 000. Therefore, for each chain $E_{bend} \sim 320\pi kT/23000 = 0.04kT$. Similarly, the rim energy E_{rim} per chain can also be calculated to be $0.1kT$. The difference between these two values would decide the equilibrium appearance of vesicles.

In block copolymer vesicles, however, another possibility is that significant corona chain segregation may occur: the long chains tend to be on the outside and the short ones on the inside. Since steric repulsion between long chains is stronger than between the short ones, a natural curvature may form to stabilize the vesicle. Thus, the maintenance of closure may not require a bending modulus to be part of the thermodynamics.[59−61]

On the basis of the free energy calculations, in principle, we can estimate the change in free energy for different micelle morphologies with increasing the selective solvent concentration. Figure 10 shows the change in total free energy (F/kT) vs acetonitrile concentration for spheres, wormlike cylinders, and vesicles in the DMF/acetonitrile system, which is only a first approximation. There are two broad concentration regions exhibiting the mixed micelle morphologies. Our calculations only partially enter these two concentration regions, since in these two regions the micelle size and geometry cannot be precisely defined. This is particularly in the case of short cylinder micelles. It is speculated that if the free energies are going to cross over, they must be at around 21 wt % between spheres and wormlike cylinders and at around 50 wt % between cylinders and vesicles.

According to the free energy changes with acetonitrile concentrations in Figure 10, we should observe morphological changes as first-order-like transitions from one type of micelle to another. Namely, only one morphology in its own concentration region, which possesses the lowest free energy, can be observed. Any other morphology with respect to this one is

Table 2. Calculated Free Energy Components and Total Micelle Free Energies at Three Selective Solvent Concentrations

	F_{core}/kT		$F_{interface}/kT$		F_{corona}/kT		F_{total}/kT	
morphology	water	AN[a]	water	AN[a]	water	AN[a]	water	AN[a]
spheres	0.5 ± 0.05	0.4 ± 0.02	52.6 ± 3.8	58.8 ± 3.5	2.8 ± 0.15	2.4 ± 0.12	56 ± 4	61.6 ± 3.82
cylinder	0.9 ± 0.1	0.7 ± 0.1	48.6 ± 2.8	43.3 ± 3.5	3.0 ± 0.1	3.3 ± 0.25	52.5 ± 3	47.3 ± 3.79
lamella	3.1 ± 0.2	1.85 ± 0.15	32.6 ± 3	24.7 ± 1.2	4.1 ± 0.3	5.6 ± 0.3	40 ± 4	32 ± 1.5

[a] AN stands for acetonitrile.

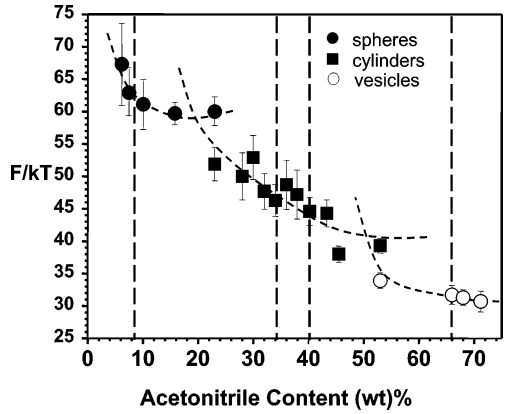

Figure 10. Free energy changes with acetonitrile content for various morphologies in the copolymer−DMF/acetonitrile system.

metastable.[62] Note that between two single morphologies there must be mixed morphologies in a narrow concentration region.[63] However, we have observed broad concentration regions exhibiting mixed morphologies. Several possibilities may exist. One is that the free energy levels of neighboring micelle morphologies are close to each other, although they do cross over; another is that the regions of mixed morphology may represent thermodynamic equilibrium.[60] Further experiments on micellization and their morphological changes at different temperatures have been designed and are being conducted to judge the explanations.

Conclusion

In summary, the micelle morphologies of PS_{962}-*b*-PEO_{227} have been studied in both DMF/water and DMF/acetonitrile systems at room temperature. TEM observations illustrate that, by adding the selective solvent (water or acetonitrile) to a copolymer solution in DMF, the micelle morphologies change from spheres to wormlike and finally to vesicles. In between two micelle morphologies, mixed morphology also exists. Morphological diagrams for PS_{962}-*b*-PEO_{227} in these two systems have been completed by determining the cmc's using light scattering experiments. Although the trend in morphological changes is identical in both these systems, a remarkable difference in the selective solvent concentrations in these two diagrams remains. The morphological changes in DMF/water system occur in a very narrow region of water concentration, while in DMF/acetonitrile they occur in a broad region of acetonitrile concentration. This difference is due to very different values of PS−solvent interaction parameters. Reversibility and annealing experiments reveal that we have obtained thermodynamic equilibrium morphologies. The micelle free energies have been quantitatively estimated as a first approximation. It has been shown that the energies decrease from spheres to wormlike cylinders and then to vesicles. Among three free energy components, the $F_{interface}$ dominates as compared to the terms of F_{core} and F_{corona}. If the free energies of two neighboring morphologies cross over, the micelle morphology change should take place as a first-order-like transition. However, in the broad selective solvent concentration regions, mixed micelle morphologies exist. This observation invites further investigations of the micelle morphology formation and changes at different temperatures.

Acknowledgment. This work was supported by NSF (DMR-0516602). Thoughtful comments and help from Professors A. Eisenberg and B. Chu are greatly appreciated.

References and Notes

(1) Whitmore, M. D.; Noolandi, J. *Macromolecules* **1985**, *18*, 657.
(2) Halperin, A. *Macromolecules* **1987**, *20*, 2943.
(3) Nagarajan, R.; Ganesh, K. *J. Chem. Phys.* **1989**, *90*, 5843.
(4) Hilfiker, R.; Wu, D. Q.; Chu, B. *J. Colloid Interface Sci.* **1990**, *135*, 573.
(5) Gast, A. P.; Vinson, P. K.; Cogan-Farinas, K. A. *Macromolecules* **1993**, *26*, 1774.
(6) Qin, A.; Tian, M.; Ramireddy, C.; Webber, S. E.; Munk, P. *Macromolecules* **1994**, *27*, 120.
(7) Antonietti, M.; Heinz, S.; Schmidt, M.; Rosenauer, C. *Macromolecules* **1994**, *27*, 3726.
(8) Glatter, O.; Scherf, G.; Schillén, K.; Brown, W. *Macromolecules* **1994**, *27*, 6046.
(9) Halperin, A.; Tirrel, M.; Lodge, T. P. *Adv. Polym. Sci.* **1992**, *100*, 31.
(10) Astafieva, I.; Zhong, X. F.; Eisenberg, A. *Macromolecules* **1993**, *26*, 7339.
(11) Gao, Z.; Varshney, S. K.; Wong, S.; Eisenberg, A. *Macromolecules* **1994**, *27*, 7923.
(12) Zhang, L.; Yu, K.; Eisenberg, A. *Science* **1996**, *272*, 1777.
(13) Zhang, L.; Eisenberg, A. *J. Am. Chem. Soc.* **1996**, *118*, 3168.
(14) Jain, S.; Bates, F. S. *Science* **2003**, *300*, 460.
(15) Putaux, J. L.; Minatti, E.; Lefebvre, C.; Borsali, R.; Schappacher, M.; Deffieux, A. *Faraday Discuss.* **2004**, *28*, 163.
(16) Geng, Y.; Ahmed, F.; Bhasin, N.; Disher, D. E. *J. Phys. Chem. B* **2005**, *109*, 3772.
(17) Alexandridis, P.; Lindman, B. *Amphiphilic Block Copolymers: Self-Assembly and Applications*; Elsevier: New York, 2000; p 305.
(18) Kim, Y.; Dalhaimer, P.; Christian, D. V.; Discher, D. E. *Nanotechnology* **2005**, *16*, S484.
(19) Allen, C.; Han, J.; Yu, K.; Maysinger, D.; Eisenberg, A. *J. Controlled Release* **2000**, *63*, 275.
(20) Chouchair, A.; Eisenberg, A. *Eur. Phys. J. E* **2003**, *10*, 37.
(21) Chen, E.; Xia, Y.; Graham, M. J.; Foster, M. D.; Mi, Y.; Wu, W.; Cheng, S. Z. D. *Chem. Mater.* **2003**, *15*, 2129.
(22) Cornelissen, J. J. J. M.; Fisher, M.; Sommerdijk, A. J. M. N.; Nolte, R. J. M. *Science* **1998**, *280*, 1427.
(23) Liu, X. Y.; Kim, J. S.; Eisenberg, A. *Macromolecules* **2005**, *38*, 6749.
(24) Zhang, L.; Eisenberg, A. *Polym. Adv. Technol.* **1998**, *9*, 677.
(25) Shen, H.; Eisenberg, A. *J. Phys. Chem. B* **1999**, *103*, 9473.
(26) Franta, E. *J. Chim. Phys.* **1966**, *63*, 593.
(27) Riess, G.; Rogez, D. *Polym. Prepr.* **1982**, *23*, 19.
(28) Bronstein, L. M.; Chernyshov, D. M.; Timofeeva, G. I.; Dubrovina, L. V.; Valetsky, P. M. *Langmuir* **1999**, *15*, 6195.
(29) Bronstein, L. M.; Chernyshov, D. M.; Timofeeva, G. I.; Dubrovina, L. V.; Valetsky, P. M.; Obolonkova, E. S.; Khokhlov, A. R. *Langmuir* **2000**, *16*, 3626.
(30) Yu, K.; Eisenberg, A. *Macromolecules* **1996**, *29*, 6359.
(31) Yu, K.; Zhang, L.; Eisenberg, A. *Langmuir* **1996**, *12*, 5980.
(32) Yu, K.; Eisenberg, A. *Macromolecules* **1998**, *31*, 3509.
(33) Yu, K.; Bartels, C.; Eisenberg, A. *Macromolecules* **1998**, *31*, 9399.
(34) Yu, K.; Bartels, C.; Eisenberg, A. *Langmuir* **1999**, *15*, 7157.
(35) Yuan, J.; Li, Y.; Li, X.; Cheng, S.; Jiang, L.; Feng, L.; Fan, Z. *Eur. Polym. J.* **2003**, *39*, 767.
(36) Quirk, R. P.; Kim, J.; Kausch, C.; Chun, M. S. *Polym. Int.* **1996**, *39*, 3.
(37) Barton, A. F. M. *Handbook of Polymer-Liquid Interaction Parameters and Solubility Parameters*; CRC Press: Boston, MA, 1990; p 12.
(38) Won, Y. Y.; Brannan, A. K.; Davis, H. T.; Bates, F. S. *J. Phys. Chem. B* **2002**, *106*, 3354.

(39) Tian, M.; Qin, A.; Ramireddy, C.; Webber, S. E.; Munk, P.; Tuzar, Z.; Prochazka, K. *Langmuir* **1993**, *9*, 1741.
(40) Based on our surface-enhanced Raman scattering experiments conducted on the micelles, the PEO blocks are on the surface as corona, and no PS blocks appear on the micelle surface.
(41) Kent, M. S. *Macromol. Rapid Commun.* **2000**, *21*, 243.
(42) Chen, W. Y.; Zheng, J. X.; Cheng, S. Z. D.; Li, C. Y.; Huang, P.; Zhu, L.; Xiong, H.; Ge, Q.; Guo, Y.; Quirk, R. P.; Lotz, B.; Deng, L.; Wu, C.; Thomas, E. L. *Phys. Rev. Lett.* **2004**, *93*, 028301.
(43) Zheng, J. X.; Xiong, H.; Chen, W. Y.; Lee, K.; Van Horn, R. M.; Quirk, R. P.; Lotz, B.; Thomas, E. L.; Shi, A.; Cheng, S. Z. D. *Macromolecules* **2006**, *39*, 641.
(44) Devanand, K.; Selser, J. C. *Macromolecules* **1991**, *24*, 5943.
(45) Lund, R.; Willner, L.; Stellbrink, J.; Radulescu, A.; Richter, D. *Macromolecules* **2004**, *37*, 9984.
(46) Zhulina, E. B.; Adam, M.; LaRue, I.; Sheiko, S. S.; Rubinstein, M. *Macromolecules* **2005**, *38*, 5330.
(47) Semenov, A. N. *Sov. Phys. JETP* **1985**, *15*, 235.
(48) Bang, J.; Jain, S.; Li, Z.; Lodge, T P.; Pedersen, J S.; Kesselman, E.; Talmon, Y. *Macromolecules* **2006**, *39*, 1199.
(49) Helfand, E.; Tagami, Y. *J. Polym. Sci., Part B* **1971**, *9*, 741.
(50) Munch, M. R.; Gast, A. P. *Macromolecules* **1988**, *21*, 1360.
(51) Rubinstein, M.; Colby, R. H. *Polymer Physics*; Oxford University Press: Oxford, UK, 2003.
(52) Hansen, P. L.; Cohen, J. A.; Podgornik, R.; Parsegian, V. A. *Biophys. J.* **2003**, *84*, 350.
(53) Venohr, H.; Fraaije, V.; Strunk, H.; Borchard, W. *Eur. Polym. J.* **1998**, *34*, 723.
(54) Duval, M.; Sarazin, D. *Polymer* **2000**, *41*, 2711.
(55) Brandrup, J.; Immergut, E. H. *Polymer Handbook*, 2nd ed.; Wiley-Interscience: New York, 1975; pp VII 38, VII 526.
(56) Elias, H. G.; Lys, H. *Makromol. Chem.* **1966**, *92*, 1.
(57) Antonietti, M.; Förster, S. *Adv. Mater.* **2003**, *15*, 1323.
(58) Oberdissea, J. *Eur. Phys. J. B* **1998**, *3*, 463.
(59) Luo, L.; Eisenburg, A. *J. Am. Chem. Soc.* **2001**, *123*, 1012.
(60) Luo, L.; Eisenburg, A. *Angew. Chem., Int. Ed.* **2002**, *41*, 1001.
(61) Liu, F.; Eisenberg, A. *J. Am. Chem. Soc.* **2003**, *125*, 15059.
(62) Keller, A.; Cheng, S. Z. D. *Polymer* **1998**, *39*, 4461.
(63) Koningsveld, R.; Stockmayer, W. H.; Nies, E. *Polymer Phase Diagrams*; Oxford University Press: New York, 2001; pp 203−207.

MA060677S